Control of nonlinear absorption and amplification of light in Er^{3+}-doped fluoroindate glass

G. S. Maciel,* N. Rakov, and Cid B. de Araújo

Departamento de Física, Universidade Federal de Pernambuco, 50670-901 Recife, Pernambuco, Brazil

Y. Messaddeq

Instituto de Química, Universidade do Estado de São Paulo, 14800-900 Araraquara, São Paulo, Brazil

Received June 18, 1999

Nonlinear absorption and amplification of a probe laser beam can be controlled by adjustment of the intensity-modulation frequency and the wavelength of a pump laser beam. A demonstration of this effect in Er^{3+}-doped fluoroindate glass is presented. The results show maximum amplification of the probe beam (~12%) when a pump laser emitting 16 mW of power is modulated at ~30 Hz. In the limit of low modulation frequencies, or cw pumping, induced absorption of the probe beam is the dominant nonlinear process. © 1999 Optical Society of America [S0740-3224(99)02811-8]

OCIS codes: 160.5690; 300.6420; 230.4320.

1. INTRODUCTION

The phenomenon whereby the intensity of a probe beam transmitted through a sample is altered by modulation of a pump beam has been studied in many ways.[1–3] This phenomenon has been investigated in media with a variety of mechanisms, for the study of light–matter interaction, and in various applications. For example, the interaction between two beams can be demonstrated in laser-induced grating experiments, such as in Kerr-like media[4] and in photorefractive materials,[5] and in cross-phase-modulation experiments.[6,7] Another important category of process is based on the effects of induced absorption or amplification owing to the coupling between two beams. Examples of this category are illustrated in Refs. 8 and 9, where saturation effects are exploited in organic materials.

In this paper we present a new way to control the intensity of a probe beam through the modulation frequency of a pump beam, its wavelength, or both. A study of optically induced modulation (OIM) of a cw laser beam transmitted through a sample of Er^{3+}-doped glass owing to the presence of another beam was performed to characterize the OIM effect. We used samples of a fluoroindate glass that is a material that has already been investigated for a variety of photonic applications such as frequency upconverters,[10–14] a temperature sensor,[15] and a laser host.[16] We investigated the efficiency of the OIM process by varying the pump laser wavelength and its intensity-modulation frequency.

2. EXPERIMENTAL PROCEDURE AND RESULTS

The sample used was a fluoroindate glass (FIG) with the following composition (in mol. %): $37\,InF_3-20\,ZnF_2-20\,SrF_2-16\,BaF_2-2\,GdF_3-2\,NaF-1\,GaF_3-2\,ErF_3$.

The glass was synthesized with standard proanalysis oxides and fluorides as the starting materials. The procedure is a classic ammonium bifluoride process. However, gallium and indium oxides are sensitive to hydrolisis during their conversion into fluorides. The fluoride powders that we used to prepare the desired compositions were then mixed together and heat treated first at 700 °C for melting and then at 800 °C for refining. The melt was finally poured between two preheated brass plates to permit the preparation of samples of different thicknesses. Fining, casting, and annealing were carried out in a way similar to that for standard fluoride glasses under a dry-argon atmosphere. The samples prepared had good chemical stability and good resistance to moisture.

Optical absorption measurements were made with a double-beam spectrophotometer. For all measurements the spectrophotometer bandwidth was smaller than the observed linewidths, which are mainly due to inhomogeneous broadening. The absorption spectrum of the sample in the visible range is presented in Fig. 1. The infrared spectrum as well as the Raman scattering spectrum of this material was presented previously.[17] It is important to recall that the small phonon energies of the FIG matrix permit longer lifetimes of the Er^{3+} electronic levels[10–13] compared with those of other commonly used glasses.[18,19] The energy-level diagram for Er^{3+}-doped FIG is shown in Fig. 2, together with the relevant transitions for the present experiments.

The OIM process was investigated in a two-color pump-and-probe experiment. The pump used was a cw dye laser that operates from 620 to 660 nm. Most of the measurements were made with the laser wavelength tuned to 650 nm, resonant with the central wavelength of the transition ${}^4I_{15/2} \rightarrow {}^4F_{9/2}$ and off resonant with the transitions ${}^4I_{9/2} \rightarrow {}^2K_{15/2}$, ${}^4I_{9/2} \rightarrow {}^4G_{9/2}$, and ${}^4I_{13/2} \rightarrow {}^4F_{5/2}$ by 157, 380, and 295 cm^{-1}, respectively. The probe beam was obtained from a cw He–Ne laser operating at 633 nm; we

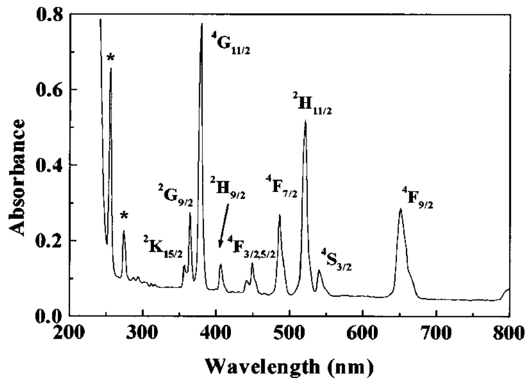

Fig. 1. Absorption spectrum. Thickness of the sample, 2.5 mm. The two peaks marked with * at 255 and 275 nm are due to Gd^{3+} present in the glass matrix.

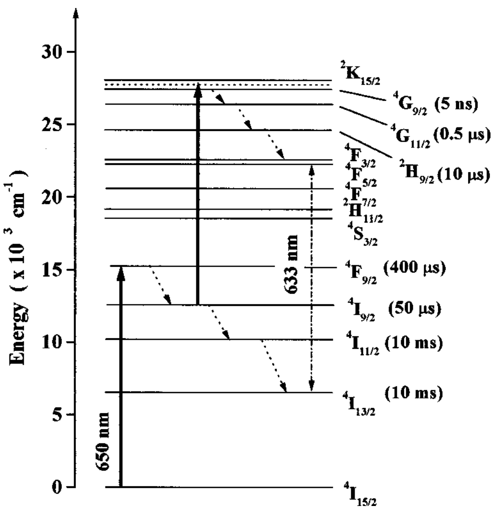

Fig. 2. Energy levels of Er^{3+} and the proposed excitation scheme. The pump laser is set on resonance with the transition $^4I_{15/2} \rightarrow {}^4F_{9/2}$ at 650 nm, and the probe beam, at 633 nm, is on resonance with the transition $^4I_{13/2} \rightarrow {}^4F_{5/2}$. The numbers in parentheses are the lifetimes of the relevant levels.

kept the laser's power below 7 μW to prevent a possible photon avalanche.[20] The He–Ne laser was chosen because its wavelength is resonant with the transition between excited states $^4I_{13/2} \leftrightarrow {}^4F_{5/2}$, as indicated in Fig. 2. The pump and the probe laser beams were collinear, and focusing of both beams in the sample was achieved with a lens of 2.5-cm focal length. The pump beam was modulated at frequency f by use of a mechanical chopper, and the OIM process was studied through the measurement of the probe beam intensity transmitted through the sample. The probe beam was monitored with a 0.5-m monochromator attached to a photomultiplier tube coupled to a digital oscilloscope.

Frequency upconversion emissions at 407 nm ($^2H_{9/2} \rightarrow {}^4I_{15/2}$), 474 nm ($^4G_{9/2} \rightarrow {}^4I_{13/2}$), 525 nm ($^2H_{11/2} \rightarrow {}^4I_{15/2}$), and 550 nm ($^4S_{3/2} \rightarrow {}^4I_{15/2}$) were observed for all modulation frequencies used and for pump wavelengths in the range 620–660 nm. The blue and green emissions have a quadratic dependence on the pump laser intensity, indicating that each photon emitted is due to the annihilation of two incident photons. The upconverted fluorescence decreased with increasing pump beam modulation frequency f, and its intensity was stronger for the pump beam wavelength in resonance with the ground-state absorption ($^4I_{15/2} \rightarrow {}^4F_{9/2}$) at 650 nm.

The behavior of the probe beam transmitted through the sample was investigated for various modulation frequencies of the pump beam. The presence of the pump beam induces intensity modulation of the probe beam, causing either absorption or amplification as it propagates through the sample. The OIM signal had the same modulation frequency f as the pump beam, and its amplitude was sensitive to the spatial overlap of the two beams. No OIM signal was detected when the probe beam was blocked, which indicates that there was no leakage of the pump beam throughout the monochromator.

Amplification of the probe beam is illustrated in Fig. 3, which shows an exponential growth of probe beam intensity as a function of pump beam power for $f = 34$ Hz. The amplitude of the amplified signal was measured as a function of f while the pump beam power was fixed at 16 mW. The results are shown in Fig. 4, the maximum OIM signal was observed near $f = 30$ Hz, corresponding to a 12% increase of the probe beam. When the pump laser

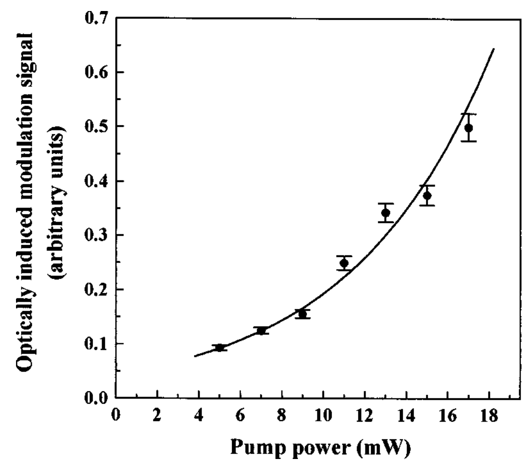

Fig. 3. OIM signal detected as a function of pump laser power at 650 nm. The intensity of the pump beam is modulated at $f = 34$ Hz. The solid curve is an exponential curve that represents the best fit with experimental data.

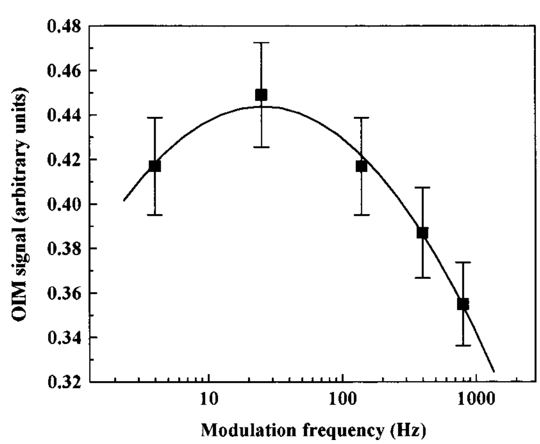

Fig. 4. OIM signal as a function of the modulation frequency of the pump beam (pump power, ~16 mW). The solid curve is the best fit of an empirical curve with the experimental data.

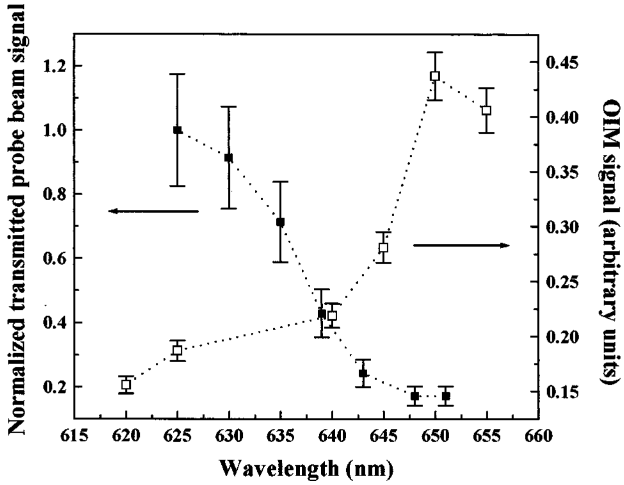

Fig. 5. Transmitted probe beam intensity (filled squares) as a function of the pump beam wavelength for a cw pumping regime and OIM signal (open squares) as a function of the pump beam wavelength for a pumping modulation frequency of 34 Hz (pump power, ~16 mW). Dashed curves are guides to the eye.

was operating in a cw regime, an induced absorption of the probe laser was observed.

We also investigated induced absorption and amplification of the probe beam when the wavelength of the pump beam was changed but its power was fixed. The results are shown in Fig. 5, which displays the behavior of the transmitted probe beam intensity when the pump beam is operating at a constant intensity and when its intensity is chopped at 34 Hz. We note that the phenomenon of amplification is more pronounced when the pump beam wavelength λ is on resonance with the transition $^4I_{15/2} \rightarrow {}^4F_{9/2}$ and that the signal decreases for $\lambda < 650$ nm as well as for $\lambda > 650$ nm.

3. DISCUSSION

The dynamics followed by the excited-state populations are responsible for the characteristics of the OIM effect, the main excitation pathways are indicated in Fig. 2. First, the pump beam creates a population in excited state $^4F_{9/2}$ followed by nonradiative decay to level $^4I_{9/2}$. Subsequently, a second pump photon is absorbed in a phonon-assisted transition from level $^4I_{9/2}$ to level $^2K_{15/2}$ or $^4G_{9/2}$. The population reaches level $^4F_{5/2}$ after multiphonon relaxation from higher-lying levels. The probe beam interrogates the population difference between levels $^4F_{5/2}$ and $^4I_{13/2}$, and, as a consequence, the OIM signal measured is the result of a balance between absorption owing to $^4I_{9/2} \rightarrow (^2K_{15/2}, {}^4G_{9/2})$ and stimulated emission corresponding to $^4F_{5/2} \rightarrow {}^4I_{13/2}$. The excitation pathway described in Fig. 2 illustrates why a decrease of the OIM signal is observed for small frequencies (Fig. 4). Indeed, for $f < 30$ Hz the pump pulse is long enough (>15 ms) for the population to reach smaller energy levels such as $^4I_{13/2}$ during the pulse interval. Hence, because of the long lifetime of level $^4I_{13/2}$ (~10 ms), there is an accumulation of population in this level and the probe photons have a probability of being absorbed from level $^4I_{13/2}$ to level $^4F_{5/2}$. Accordingly, in the cw regime of excitation the absorption process dominates, and thus a reduction in the transmitted intensity of the He–Ne beam is observed. Also, we observed strong nonlinear absorption of the pump beam in one-beam experiments with cw excitation.[21] Analogous reasoning explains why the OIM signal becomes weaker for increasing f. The second pump photon is absorbed only after the population initially deposited in level $^4F_{9/2}$ reaches level $^4I_{9/2}$. The lifetime of level $^4F_{9/2}$ is ~400 μs,[22] which implies that for modulation frequencies in the range 30 Hz–1.25 kHz the population at level $^4I_{9/2}$ will be negligible. Consequently, the OIM signal is minimized because of the weak absorption through $^4I_{9/2} \rightarrow (^2K_{15/2}, {}^4G_{9/2})$ during the time interval in which the pump laser is present. For higher modulation frequencies, $f > 1.25$ kHz, the pump beam can be considered cw because the intensity modulation is faster than any characteristic time involved in the process. Therefore, strong absorption at either fast modulation frequencies or cw pumping should be expected, based on the results found in the one-beam experiment.[21] The absorption cross sections of the excited-state transitions have to be higher than the absorption cross section of the ground-state transition for the nonlinear absorption to be efficient.[23] Indeed, the absorption cross section of the transition $^4I_{13/2} \rightarrow {}^4F_{5/2}$ is five times larger than the cross section of transition $^4I_{15/2} \rightarrow {}^4F_{9/2}$,[24] and the nonlinear absorption process was well described by a model based on coupled nonlinear rate equations for the level's population.[21]

For practical applications it is important to measure β, the nonlinear coefficient of the material, and the OIM signal amplitude can be used to estimate its value. Hence the propagation of the probe beam with intensity I_1 through the nonlinear medium, in the presence of a strong pump beam with intensity I_2, can be described by

$$\frac{\mathrm{d}I_1(z)}{\mathrm{d}z} = -\alpha_1 I_1(z) + \beta I_2{}^2(z) I_1(z), \tag{1}$$

where z is the position along the propagation direction.

The solution to Eq. (1) for the transmitted intensity is given by

$$I_1(d) = (1 - R)^2 \exp(-\alpha_1 d) I_1(0) \exp\{\beta(1 - R)^2 I_2{}^2(0) \times [1 - \exp(-2\alpha_2 d)]/2\alpha_2\}, \tag{2}$$

where α_1 and α_2 are the linear absorption coefficients at the probe and the pump beam wavelengths, respectively, R is the reflectivity at the sample's surfaces, d is the sample thickness, and $I_2(0)$ is the intensity of the pump beam just before the beam enters the sample. The nonlinear term in Eq. (1) arises because the intensity of the probe beam is affected by the presence of the pump beam, and the quadratic dependence on I_2 comes from the fact that two photons of the pump beam are necessary to begin the nonlinearity. When the pump beam is off, $I_2(0) = 0$, we obtain

$$I_1{}^0(d) = (1 - R)^2 \exp(-\alpha_1 d) I_1(0). \tag{3}$$

Therefore the value of β can be determined from Eqs. (2) and (3). The ratio $I_1(d)/I_1{}^0(d)$ is proportional to the OIM signal, as shown in Fig. 3, and we found that $\beta = (3.6 \pm 0.2) \times 10^{-8}\ \mathrm{cm^3/W^2}$ for a pump intensity-modulation frequency of 34 Hz. The parameters used were $I_2(0) = 4.5 \times 10^3$ W/cm^2 (pump power, 17 mW), $\alpha_2 = 2.71\,\mathrm{cm}^{-1}$, $d = 1.25\,\mathrm{cm}$, and $R = 0.04$. The nonlinear coefficient β depends on modulation frequency f, as illustrated in Fig. 4, and can be calculated for each value of f by the same procedure.

4. CONCLUSIONS

In summary, we observed optically induced modulation corresponding to nonlinear absorption or amplification of a probe beam at 633 nm in resonance with excited states of erbium ions in a fluoroindate glass. The excitation source was a dye laser tuned about the transition ${}^4I_{15/2} \rightarrow {}^4F_{9/2}$ of Er^{3+}. The efficiency of the process was studied as a function of the modulation frequency of the pump laser intensity, and the results show maximum amplification of the probe beam (~12%) when the pump laser emitting 16 mW of power is modulated at ~30 Hz. In the limit of low modulation frequencies, or cw pumping, induced absorption of the probe beam is the nonlinear process, which dominates. One can control the degree of absorption induced in the probe beam by tuning the pump beam near 650 nm to be in resonance with a transition originating from the ground state of Er^{3+}.

ACKNOWLEDGMENT

Partial financial support from the Brazilian agencies Conselho Nacional de Desenvolvimento Científico e Tecnológico, Coordenaçáo de Aperfeicoamento de Pessoal de Nível Superior, and Financiadora de Estudos e Projetos/ Programa de Nucleos de Excelência is acknowledged.

*Present address, Natural Sciences Complex, State University of New York, Buffalo, New York, 14260-3000.

REFERENCES

1. H. M. Gibbs, *Optical Bistability: Controlling Light by Light* (Academic, New York, 1985).
2. G. P. Agrawal, *Nonlinear Fiber Optics* (Academic, New York, 1995).
3. A. Miller, D. A. B. Miller, and S. D. Smith, "Dynamic nonlinear optical processes in semiconductors," Adv. Phys. **30**, 697–800 (1981).
4. H. J. Eichler, P. Günther, and D. W. Pohl, *Laser Induced Dynamic Gratings*, Vol. 50 of Springer Series in Optical Sciences (Springer-Verlag, Berlin, 1986).
5. A. Brignon and J. P. Huignard, "Continuous-wave operation of saturable-gain degenerate four-wave mixing in a Nd:YVO_4 amplifier," Opt. Lett. **20**, 2096–2098 (1995).
6. S. Matsuoka, N. Miyanaga, S. Amano, and M. Nakatsuka, "Frequency modulation controlled by cross-phase modulation in optical fiber," Opt. Lett. **22**, 25–27 (1997).
7. D. J. Hagan, Z. Wang, G. Stegeman, E. W. Van Stryland, M. Sheik-Bahae, and G. Assanto, "Phase-controlled transistor action by cascading of second-order nonlinearities in KTP," Opt. Lett. **19**, 1305–1307 (1994).
8. M. J. Damzen, K. J. Baldwin, and P. J. Soan, "Optical switching and high-resolution image transfer in a saturable dye spatial light modulator," J. Opt. Soc. Am. B **11**, 313–319 (1994).
9. A. Peda'el, R. Daisy, M. Horowitz, and B. Fischer, "Beam coupling-induced transparency in a bacteriorhodopsin-based saturable absorber," Opt. Lett. **23**, 1173–1175 (1998).
10. G. S. Maciel, C. B. de Araújo, Y. Messaddeq, and M. A. Aegerter, "Frequency upconversion in Er^{3+}-doped fluoroindate glasses pumped at 1.48 μm," Phys. Rev. B **55**, 6335–6342 (1997).
11. L. de S. Menezes, C. B. de Araújo, G. S. Maciel, and Y. Messaddeq, "Continuous wave ultraviolet frequency upconversion due to triads of Nd^{3+} ions in fluoroindate glass," Appl. Phys. Lett. **70**, 683–635 (1997).
12. L. E. E. de Araújo, A. S. L. Gomes, C. B. de Araújo, Y. Messaddeq, A. Florez, and M. A. Aegerter, "Frequency upconversion of orange light into blue light in Pr^{3+} doped fluoroindate glasses," Phys. Rev. B **50**, 16219–16223 (1994).
13. E. M. Pacheco, C. B. de Araújo, and Y. Messaddeq, "Energy transfer between Pr^{3+} ions in a fluoroindate glass," J. Non-Cryst. Solids **226**, 265–272 (1998).
14. S. Kishimoto and K. Hirao, "Intense ultraviolet and blue upconversion fluorescence in Tm^{3+}-doped fluoroindate glasses," J. Appl. Phys. **80**, 1965–1969 (1996).
15. G. S. Maciel, L. de S. Menezes, A. S. L. Gomes, C. B. de Araújo, Y. Messaddeq, and M. A. Aegerter, "Temperature sensor based on frequency upconversion in Er^{3+}-doped fluoroindate glass," IEEE Photonics Technol. Lett. **7**, 1474–1476 (1995).
16. J. Azkargorta, I. Iparraguirre, R. Balda, J. Fernández, E. Dénoue, and J. L. Adam, "Spectroscopic and laser properties of Nd^{3+} in BIGaZLuTMn fluoride glass," IEEE J. Quantum Electron. **30**, 1862–1867 (1994).
17. R. M. Almeida, J. C. Pereira, Y. Messaddeq, and M. A. Aegerter, "Vibrational spectra and structure of fluoroindate glasses," J. Non-Cryst. Solids **161**, 105–108 (1993).
18. See, for example, M. J. Digonnet, ed., *Rare-Earth Doped Fiber Lasers and Amplifiers* (Marcel Dekker, New York, 1993), and references therein.
19. X. Zou and T. Izumitami, "Spectroscopic properties and mechanism of excited state absorption and energy transfer upconversion for Er^{3+}-doped glasses," J. Non-Cryst. Solids **162**, 68–80 (1993).
20. N. Rakov, C. B. de Araújo, Y. Messaddeq, and M. A. Aegerter, "Avalanche upconversion in Er^{3+}-doped fluoroindate glass," Appl. Phys. Lett. **70**, 3084–3086 (1997).
21. C. B. de Araújo, G. S. Maciel, N. Rakov, and Y. Messaddeq, "Giant nonlinear absorption in Er^{3+}-doped fluoroindate glass," J. Non-Cryst. Solids **247**, 209–214 (1999).
22. T. Catunda, L. A. O. Nunes, A. Florez, Y. Messaddeq, and M. A. Aegerter, "Spectroscopic properties and upconversion mechanisms in Er^{3+}-doped fluoroindate glasses," Phys. Rev. B **53**, 6065–6070 (1996).
23. L. W. Tutt and T. F. Boggess, "A review of optical limiting mechanisms and devices using organics, fullerenes, semiconductors and other materials," Prog. Quantum Electron. **17**, 299–338 (1993).
24. G. S. Maciel, "Nonlinear spectroscopy of fluoroindate glasses and polymers," Ph.D. dissertation (Universidade Federal de Pernambuco, Recifer, Brazil, 1999).